

Dead Zones and Extrasolar Planetary Properties

Soko Matsumura^{1*} and Ralph E. Pudritz^{1,2}

¹*Department of Physics and Astronomy, McMaster University, 1280 Main Street West, Hamilton, ON, L8S 4M1, Canada*

²*Origins Institute, ABB 241, McMaster University, 1280 Main Street West, Hamilton, ON, L8S 4M1, Canada*

ABSTRACT

Most low-mass protostellar disks evolve in clustered environments where they are affected by external radiation fields, while others evolve in more isolated star-forming regions. Assuming that the magneto-rotational instability (MRI) is the main source of viscosity, we calculate the size of a poorly ionized, MRI inactive, and hence low viscosity region – the “dead zone” – in these protostellar disks. We include disk ionization by X-rays, cosmic rays, radioactive elements and thermal collisions, recombination by molecules, metals, and grains, as well as the effect of turbulence stimulation in the dead zone by the active layers lying above it. We also calculate the gap-opening masses of planets, which are determined by a disk’s viscosity and a disk aspect ratio, for disks in these environments and compare them with each other.

We find that the dead zone is a robust feature of the protostellar disks that is largely independent of their environment, typically stretching out to ~ 15 AU. We analyze the possible effects of dead zones on planet formation, migration, and eccentricity evolution. We show that the gap-opening mass inside the dead zone is expected to be of the order of terrestrial and ice giant mass planets while that outside the dead zone is Jovian or super-Jovian mass planets, largely independent of the star-forming environment. We show that dead zones can significantly slow down both type I and type II planetary migration due to their lower viscosity. We also find that the growth of eccentricity of massive extrasolar planets is particularly favorable through the planet-disk interaction inside the dead zones due to the large gaps expected to be opened by planets.

Key words: accretion, accretion disks - turbulence - planetary systems: formation - planetary systems: protoplanetary disks - planets and satellites: general - Solar system: formation - stars: pre-main-sequence

1 INTRODUCTION

The discovery of over 160 extrasolar planets has opened up several fundamental questions about planet formation. Planetary masses vary from 7.5 Earth masses all the way up to ~ 15 Jupiter masses. Massive planets are found close to their central stars which implies that their migration from their points of origin further out in the disk needs to be understood. The high eccentricity of many of the planets also demands explanation. Theoretical attention has increasingly focused on the interaction of planets and their surrounding disks in order to elucidate these questions. In this regard, while most models still assume that disks possess a constant turbulent viscosity throughout, the possibility that “dead zones” of very low turbulence exist in disks has profound effects on planet formation (Matsumura & Pudritz 2003, hereafter MP03).

The idea of a dead zone in protostellar disks was first proposed by Gammie (1996). He argued that there is a poorly ionized region where the growth of the magneto-rotational instability (MRI) against Ohmic dissipation cannot be sustained. Since the MRI is thought to be the most promising source of the disk’s turbulent “viscosity”, the dead zone is expected to have nonzero, but very low viscosity.

Dead zones have several important effects on planet formation including (1) planetary masses, (2) planetary migration, (3) planet formation via gravitational instability, and (4) planetary eccentricity. We discuss these below.

The first point was analyzed in our previous paper (Matsumura & Pudritz 2005, hereafter MP05): the gap-opening mass of planets is expected to be smaller inside the dead zone. A planet opens a gap when the angular momentum transfer rate by the planetary tidal torque exceeds that of the disk’s viscous torque (e.g. Lin & Papaloizou 1993). Since a dead zone has a very low viscosity, the gap-clearing timescale is sufficiently short compared to the gas-accretion

* E-mail: soko@physics.mcmaster.ca (SM); pudritz@physics.mcmaster.ca (REP)

timescale in that region so that a planet won't accrete much gas.

Regarding the second point, dead zones are likely to prolong the planetary migration timescale (e.g. Chiang et al. 2002, MP05). This is potentially important because the migration timescale estimated in a protostellar disk without a dead zone tends to be much shorter than a disk's lifetime, and as yet we have no obvious mechanism to stop planet migration. Protoplanets migrate as a result of their resonant interaction with protostellar disks. They tend to migrate inward because the magnitude of the outer torque is usually larger than the inner torque (Ward 1997). The current theories suggest that planetary migration has essentially two stages. The first stage is when protoplanets are not massive enough to open a gap in the disk; they migrate through the disk (type I) as they accumulate mass. The second stage starts when protoplanets become sufficiently massive to open a gap; they migrate at the viscous timescale of the disk (type II) without accumulating much mass. A dead zone can affect both types of migration. A dead zone's effect on type II migration can be readily understood – a planet's migration speed is significantly slowed down as soon as they enter a dead zone. This is because the speed of type II migration is directly proportional to a disk's viscosity and because the viscosity in a dead zone is expected to be very low.

A dead zone's effect on type I migration is rather indirect – planet migration can be halted or even reversed by the mass accumulation at the edge of the dead zone (e.g. Thommes 2005). Even when planets are not stopped at the edge of the dead zone, their migration speed is still likely to be reduced as soon as they enter it. This is because these planets will probably open gaps in the dead zone where the gap-opening mass is roughly a couple of orders of magnitude smaller. These planets then switch to the type II migration that is a few orders of magnitude slower than the type I migration (Ward 1997). Thus, the dead zone may rescue planets from plunging into the central star due to its lower viscosity, and may also work as a switch from type I to type II migrations or even as a wall to halt or reverse the type I migration. We will further discuss this point in §5.

Regarding the third point, the mass accumulation at the edge of a dead zone, or even at the edge of a gap opened by a planet, may lead to planet formation via gravitational instability, which requires a dense, cold region (e.g. Boss 1997; Mayer et al. 2002). The former type of mass accumulation occurs due to different evolution speeds between dead zones and active zones, while the latter mass accumulation happens because the gap-opening timescale tends to be faster than the disk's viscous evolution timescale. Lufkin et al. (2004) showed that higher density spiral arms formed by a massive planet can lead to a subsequent planet formation by gravitational instability.

Regarding the fourth and final point, we propose in this paper that the dead zone may be an optimum place for the eccentricity evolution, especially for a disk-planet interaction scenario proposed by Goldreich & Sari (2003). The lower viscosity inside the dead zone would make a wider gap around a planet, and therefore allow more space and time for eccentricity growth. We discuss this point in §6.

In this paper, we generalize our work in MP05 and calculate the size of dead zones and planetary gap-opening masses in regions of clustered and isolated star-forming en-

vironments. This allows us to examine how much the size of dead zones is changed by its environment, and therefore which parameters affect them most. We also discuss each possible effect of a dead zone proposed above. We find that both the size of a dead zone (typically $\sim 10 - 20$ AU) and gap-opening masses are almost independent of a disk's environment. This is because the disk structures and hence the ionization structures in dense regions of disks (e.g. a possible region of a dead zone) are almost the same for both isolated and clustered star-forming environments. We give an overview of a gap-opening mass in §2, and the MRI turbulence and our disk models in §3. We present our results in §4 and discuss dead zone effects on migration and eccentricity growth in §5 and §6 respectively. Finally, we summarize our work in §7.

2 GAP-OPENING MASS

The mechanisms of angular momentum transfer in protostellar disks are not fully understood, but planet formation is thought to be linked to at least two of them – tidal interaction between a gaseous disk and a protoplanet, and viscous diffusion of a disk.

Tidal torques carry away angular momentum most efficiently around Lindblad resonances located at about a disk pressure scale height h from a protoplanet (Goldreich & Tremaine 1980) and transfer that to the disk when generated density waves shock and damp. Assuming the disk is inviscid so that there is no viscous torque, and that the density waves shock immediately in the vicinity of the Lindblad resonances, Lin & Papaloizou (1993) determined a gap-opening mass of the planet:

$$\frac{M_p}{M_*} \geq 3 \left(\frac{h_p}{r_p} \right)^3, \quad (1)$$

where M_p and M_* are mass of a planet and a star respectively, r_p is the orbital radius of the planet, and h_p is the pressure scale height at that radius. Rafikov (2002) argued that their assumption is too radical and determined the gap-opening mass in an inviscid disk by considering the nonlinear evolution of density waves as well as taking account of the planet migration effect:

$$\frac{M_p}{M_*} > \frac{2}{3} \left(\frac{h_p}{r_p} \right)^3 \min \left[5.2Q^{-5/7}, 3.8 \left(Q \frac{r_p}{h_p} \right)^{-5/13} \right], \quad (2)$$

where Q is the Toomre parameter. The first term represents the case of feedback being not strong enough to stop migration – the density waves reflected from the edge of a forming gap are not enough to fill in the gap and hence smooth out the difference between outer and inner planetary torques. The second term corresponds to the case of feedback being sufficient to stop migration. All the disk models we used turn out to be gravitationally stable ($Q \gg 1$), thus planets are expected to form through the core accretion rather than the gravitational instability, and hence have smaller gap-opening masses compared to Equation (1). Equation (1) replaces Equation (2) when density waves damp immediately at the Lindblad resonances (at a distance of $\sim h_p$ from the planet) where they are excited.

When the disk is viscous, we need to take account of

the effect of viscous torque whose primary source is thought to be the MRI turbulence. Balbus & Hawley (1991) showed that a slightly perturbed, weak magnetic field can be amplified sufficiently to radially transfer the angular momentum. Recent numerical simulations (e.g. Fleming et al. 2000) have shown that the MRI is active when the dissipation timescale of the turbulence ($t_{dis} = h^2/\eta$) is more than $10^3 - 10^4$ times slower than the growth timescale ($t_{growth} = h/V_A$):

$$Re_M = \frac{V_A h}{\eta} > 10^3 - 10^4, \quad (3)$$

where V_A is the Alfvén speed and η is the diffusivity of the magnetic field.¹

In a viscous disk, the gap-opening mass is reached when the angular momentum transfer rate by the tidal torque exceeds that by the viscous torque (e.g. Lin & Papaloizou 1993):

$$\frac{M_p}{M_*} \geq \sqrt[5]{40\alpha_{ss} \left(\frac{h_p}{r_p}\right)^5}, \quad (4)$$

where α_{ss} is the viscous α parameter (Shakura & Sunyaev 1973). For a less viscous disk, or equivalently, a disk with a smaller α_{ss} , a planetary gap-opening mass becomes smaller. Assuming that the gap-opening mass inside the dead zone is well approximated by the gap-opening equation (2), MP05 showed that the gap-opening mass ratio inside the dead zone to outside it could be up to about 100 – close to the mass ratio of Jovian to terrestrial planets in our solar system.

Although numerical simulations show that there is some residual gas accretion through a gap (e.g. Kley 1999; Lubow et al. 1999), the gap-opening mass is still expected to be close to a planet’s final mass. Kley (1999) showed that the gas accretion through a gap is markedly reduced for a small viscosity: $\alpha_{ss} \leq 5 \times 10^{-4}$. This corresponds to a viscosity inside a dead zone found in numerical simulations (e.g. Fleming & Stone 2003). Thus, we can expect that the gap-opening mass is most likely to be the final planetary mass inside a dead zone. In a standard disk with mass of $\sim 0.02M_\odot$, Lubow et al. (1999) showed that the gas accretion rate through a gap is $10^{-5} - 10^{-6} M_J/\text{year}$ at 10–40 AU – it takes $10^5 - 10^6$ years to double a mass of Jupiter outside a dead zone. This may be shorter than the disk lifetime, but longer than the planetary migration timescale in this region – type I migration timescale for Jupiter is $10^3 - 10^4$ years and type II migration timescale for $\alpha_{ss} = 0.01$ is $10^4 - 10^5$ years (see Fig. 10). Thus, as long as planets migrate inward, they probably enter a dead zone and thereby stop gas accretion (as they open a clear gap) before they acquire a significant amount of mass through gaps.

¹ Sano & Stone (2002) (hereafter SS02) studied the nonlinear evolution of the MRI in weakly ionized accretion disks including the Hall effect, and obtained the critical magnetic Reynolds number of $Re_{M,SS02} = V_A^2/(\eta\Omega) \sim 30$. Our definition of the magnetic Reynolds number relates to theirs as $Re_{M,SS02} = V_A/c_s Re_M = \alpha_{ss}^{1/2} Re_M$, where c_s is the sound speed. Therefore, their critical magnetic Reynolds number roughly corresponds to the case of $Re_M = 10^2$ for the standard viscosity parameter $\alpha_{ss} = 0.01$.

3 MRI AND DISK MODELS

3.1 MRI – its existence and effectiveness

Although the MRI is considered to be an effective potential source of disk viscosity, its existence and effectiveness are still under discussion. Regarding the former point, Fromang et al. (2002) pointed out that a very small fraction of the cosmic abundance of metal atoms can significantly diminish the size of a dead zone by picking up the charges of molecular ions which recombine with electrons 10^5 times more effectively than metal ions (i.e. keeping the overall ionization rate high). The electron fraction, however, can be significantly reduced by grains (e.g. Sano et al. 2000) because they recombine with electrons even more efficiently than molecular ions. This effect can potentially make the midplane region of an entire protostellar disk MRI dead. We consider recombination rates of electrons with metal ions, molecular ions as well as grains as in MP05 (also see Appendix A in this paper). To calculate the ionization rates, we take account of X-rays, cosmic rays, radioactive elements and thermal collisions of alkali ions (for details, see MP03 & MP05).

Dead zones have been studied by many authors both analytically (e.g. Gammie 1996; Sano et al. 2000; Glassgold et al. 2000; Fromang et al. 2002, MP03, MP05) and numerically (e.g. Fleming & Stone 2003). Recently, Inutsuka & Sano (2005) suggested that once MRI turbulence becomes active, it can be sustained in a protostellar disk without any external ionization and concluded that most regions in protostellar disks remain magnetically active. For dense regions of a disk with dust grains, they proposed that collisions of energetic electrons might provide enough ionization to sustain MRI. In considering their arguments however, we note that their estimate for the electron fraction is still one to two orders of magnitude smaller than the one required by recent numerical work. For a disk surface, assuming dust grains are depleted from the region, they proposed that turbulent eddies could mix the ionized region with the neutral region, and therefore homogenize the ionization region, if the recombination rate is sufficiently low. Grains could indeed be absent in a high temperature region close to the central star (see §4.3). However, both their effective electron recombination coefficient and the initial electron fraction are one to two orders of magnitude too small because of their assumption that $\alpha_{ss} = 0.2$.² Thus, we consider these processes are probably unable to sustain the MRI turbulence throughout the entire disk.

Even if the MRI is present, other effects like ambipolar

² Using the formula given in Inutsuka & Sano (2005), the effective recombination coefficient can be written as $\beta' \sim 10^{-7} \frac{n_{m+}}{n_e} + 10^{-12} \frac{n_{M+}}{n_e}$, where n_e , n_{m+} , and n_{M+} are number densities of electrons, molecular ions, and metal ions respectively (see Appendix A). At regions close to the central star, densities of electrons and metal ions are about two orders of magnitude larger than the density of molecular ions (Sano et al. 2000). This will give $\beta' \sim 10^{-9}$ and the electron fraction of $\sim 10^{-14}$ (see eq. (12) in Inutsuka & Sano 2005), unless the initial electron fraction is larger. Also, their suggested electron fraction to sustain MRI is likely an underestimate because they adopted a relatively large viscosity parameter $\alpha_{ss} = 0.2$.

diffusion could work against its angular momentum transport. Using three-dimensional magneto-hydrodynamic simulations, Hawley & Stone (1998) showed that there is significant angular momentum transfer when the ion-neutral collision rate is 100 times larger than the local epicyclic frequency, and that ions and neutrals are essentially decoupled when this ratio goes below 0.01. We calculated the corresponding ratio in our disk models and found that the value is typically ~ 10 . Therefore, we expect at least some angular momentum transport in active regions of our disk models.

Fleming & Stone (2003) studied the evolution of the MRI in stratified accretion disks and found that there is a minimum level of angular momentum transport in the dead zone in the presence of active layers due to the Reynolds stress. In the case relevant to ours ($\Sigma_{DZ}/\Sigma_{ALs} \sim 10$), they obtained $\alpha_{ss} \sim 10^{-3}$ for active layers and $\alpha_{ss} \sim 5 \times 10^{-5}$ for a dead zone. Later we will show that this α_{ss} value doesn't affect the gap-opening mass inside the dead zone. Another effect discussed in the literature is the mass mixing between a dead zone and the active layers lying above it (Fleming & Stone 2003). Although this vertical mixing may have no effect in radial angular momentum transfer, we take account of this effect by imposing the condition $\Sigma_{DZ}/\Sigma_{ALs} \geq 10$ on a dead zone besides $Re_M < 10^3 - 10^4$.

3.2 Disk Models – Clustered vs Isolated Star Formation

Typical protostellar systems are expected to form in a cluster like Orion Nebula, where they are irradiated by nearby luminous OB stars. On the other hand, some star formation regions like Taurus are known not to have young massive stars (e.g. Luhman et al. 2003). It is interesting to compare these two star formation regions from the viewpoint of their planet formation environments.

To determine the size of dead zones of disks in these environments, we need to calculate Re_M (see equation (3)) throughout disks that depends both on the thermal structure of the disks via h and on the ionization structure via η . Both of these quantities will be affected by the presence of massive stars.

The difference in the thermal structure for protostellar disks in the clustered and isolated case is that the former disks are exposed not only to their central stars, but also to other massive stars in the cluster. For the isolated disks, as in MP03, we adopted the isolated, two-layered disk models developed by Chiang et al. (2001). For the disks in a cluster, as in MP05, we used the disk models by Robberto et al. (2002) where they modified the isolated two-layered disk models of Chiang & Goldreich (1997) by submerging these disks in a cluster environment. In their model, the external star is assumed to be located at an average distance of 0.1 pc from a low-mass protostellar disk and have a stellar luminosity of $L_* = 6 \times 10^{38}$ ergs s^{-1} . Due to this extra heating, the disks in a cluster are more flared compared to the isolated cases (see Fig. 1). In both disk models, disk temperatures are calculated by assuming a radiative, hydrostatic equilibrium. For a particular disk radius, these models give two temperatures – one in the surface layer, and the other in the disk interior. Also, both disk models assume a power-law surface mass density: $\Sigma = \Sigma_0 \left(\frac{r}{\text{AU}}\right)^{-3/2}$.

Fig. 1 compares temperatures of these models (left panel) as well as corresponding disk aspect ratios (right panel). From the left panel, it is apparent that the disk interior temperatures (i.e. the mid-plane temperatures) are the same for both environments out to ~ 10 AU, while the radiation from external fields clearly affect on a disk's thermal structure beyond ~ 10 AU, giving a nearly constant temperature (~ 50 K) there. The temperature difference of up to a factor of ~ 2 leads to a more flared disk, and hence a larger disk aspect ratio and larger gap-opening masses in a clustered star-forming environment (see Equation (2) and (4)). From the right panel, we can see that, at 20 AU, the disk aspect ratio for isolated and clustered star-forming regions are 0.09 and 0.15 respectively. This ~ 70 % difference in a disk aspect ratio leads to a gap-opening mass of 0.8 and $1.2M_J$ (where M_J is a mass of Jupiter) in each environment for a standard alpha parameter of $\alpha_{ss} = 0.01$ (see also: Fig. 7). Note that, by knowing the radial temperature structure of the disk, and hence its aspect ratio; h/r , the only parameter needed to determine the distribution of gap-opening masses is a disk's viscosity parameter α_{ss} . We will discuss this in §4.1 and 4.2. Also, the temperature at the innermost disk reaches ~ 1500 K, suggesting that the region may be void of dust grains due to thermal evaporation. We will consider this effect in §4.3.

Note that, although the estimated surface layer's temperature of the disk model in a clustered environment is very low; ~ 200 K beyond 10 AU, compared to the atmosphere temperature assumed for photoevaporating disk models; $\sim 10^4$ K (e.g. Shu et al. 1993; Hollenbach et al. 1994), it does not affect our results so much. This is because the disk atmosphere reaches that high temperature only in very high altitude regions – about one order of magnitude higher than our surface disk height, where the density is very low. In addition, the gap-opening masses depend on the disk interior temperature, which is related to the pressure scale height rather than the disk surface temperature.

The difference in the ionization structure for protostellar disks in the clustered and isolated case is that the former is also exposed to the X-ray radiation from an external star besides other ionization sources common in both cases (see below). Here, we assume the X-ray luminosity of an external star to be $L_x = 10^{34}$ ergs s^{-1} , which is likely to be an upper limit (Stelzer et al. 2005).³ In both environments, the ionization of disks is due to X-rays from the central star ($L_x = 10^{30}$ ergs s^{-1} with $kT_x = 2$ keV, Feigelson et al. (2002)), cosmic rays ($\xi_{CR} \sim 10^{-17}$ s^{-1} with the attenuation length of ~ 96 g cm^{-2} , Sano et al. (2000)), radioactive elements ($\xi_{RA} \sim 6.9 \times 10^{-23}$ s^{-1} , Umebayashi & Nakano (1981)), as well as heated alkali ions (important in the high temperature, inner part of the disks).

³ We performed the simulation with a more typical value of the X-ray luminosity of a massive star: $L_x = 10^{31}$ ergs s^{-1} , and found that the external star has less effect on the total ionization rate. But this does not change the extent of the dead zones.

4 DEAD ZONES AND GAP-OPENING MASSES

In this section, we compare protostellar disks in different environments and obtain sizes of their dead zones (§4.1) as well as the gap-opening masses of planets (§4.2). Our focuses are on comparing (1) disks in a stellar cluster and isolated disks, and (2) disks with and without cosmic ray ionization. The latter case is included because low energy cosmic rays, which are more responsible for ionization compared to higher energy cosmic rays (e.g. Lepp 1992), may be partially excluded from the disks by magnetic scattering (Skilling & Strong 1976). Note, however, that Desch et al. (2004) recently showed that galactic cosmic ray radiation is likely to be abundant in protostellar disks. Here we include this comparison for completeness. In the end of this section, we also discuss the effect of dust evaporation (§4.3).

4.1 Clustered vs Isolated Star Formation – Dead Zones

Fig. 2 shows dead zones in all representative cases of our study – disks in a cluster, isolated disks, and disks with dead zones estimated by X-ray ionizations alone for each environment. Although we cover a large parameter space: the surface mass density of $\Sigma_0 = 10^3 - 10^4 \text{ g cm}^{-2}$, the magnetic Reynolds number of $Re_M = 10^2 - 10^4$ and $\alpha_{ss} = 1.0 - 0.001$, we only show the case of $(Re_M, \alpha_{ss}) = (10^3, 0.1 - 0.001)$ with $\Sigma_0 = 10^3 \text{ g cm}^{-2}$ in this figure. We will discuss the effects of different parameters below (see Fig. 3 as well).

Comparing disks in a cluster with isolated disks (upper two panels), we find that dead zones stretch out to $\sim 10 - 20$ AU in both environments. This is not so surprising because the effect of an external star and a nebular environment is not dominant within ~ 10 AU (see Fig. 1). The insensitivity of the dead zone size to thermal environments suggests that protostellar disks in both environments have a similar transition radius of disk’s viscosities.

Comparing the dead zones estimated by the total ionization (upper panels in Fig. 2) with those estimated by the X-ray ionization (lower panels), we can see that cosmic rays have a large effect on a dead zone shape at outer radii. Disks ionized by both X-rays and cosmic rays (as well as other sources) have fully magnetically active regions beyond ~ 10 AU, while disks ionized by X-rays alone are expected to be able to sustain MRI only when there is a significant mass-mixing between active and dead zones (note that the dashed line represents a critical surface mass density ratio of the dead zone and the active layers below which mass-mixing between these two zones is not negligible). This is essentially due to the geometrical difference between these two major ionizing sources, X-rays from a central star and cosmic rays: X-rays are emitted from a stellar magnetosphere and therefore penetrate disks with an angle of $\ll 90^\circ$. As a result, disks become more optically thick toward the outer part of a disk for X-rays. Cosmic rays on the other hand, will propagate down to the disk preferentially along disk’s magnetic field lines that are orthogonal to the disk’s surface, hit the disk with an angle of $\sim 90^\circ$ and experience a similar optical thickness throughout the disk.

As described in MP05, we define edges of the dead zones as intersections of a critical surface mass density ra-

tio (dashed line) with curved boundaries of dead zones. The dead zone edges obtained this way are plotted in Fig. 3, where we can compare parameters’ effects on the dead zone sizes in different environments and ionization sources. In a standard parameter range $(Re_M, \alpha_{ss}) = (10^3 - 10^4, 0.1 - 0.001)$, dead zones estimated by the total ionization (upper two panels) tend to be about $< 10 - 20$ % larger for disks in isolated environments. For Re_M and α_{ss} , the size of dead zones changes by about a factor of 2 each over three orders of magnitude. The most significant effect however comes from a surface mass density of the disk at 1 AU Σ_0 , for which the dead zone’s size changes by the same factor, 2, over one order of magnitude.

The difference in a dead zone size due to environments becomes more apparent for disks ionized only by X-rays (lower two panels). This is because of the extra X-ray ionization effect by a nearby massive star in a clustered star-formation region. In a relatively heavy disk with $\Sigma_0 = 10^4 \text{ g cm}^{-2}$, dead zones of isolated disks are up to about a factor of 2 larger than those of disks in a cluster. For Re_M and α_{ss} , the size of dead zones changes by about a factor of 2 and 1.5 respectively over three orders of magnitude, while for Σ_0 , the dead zone size changes by a factor of > 3 over just one order of magnitude. Thus, the environmental effect becomes more important if cosmic rays are excluded from the disks. Note however, that our estimated X-ray ionization rate for a clustered environment is probably overestimated, since we have not taken account of any extinction for X-rays traveling to the protostellar disk and since the adopted X-ray luminosity for the massive external star is likely to be an upper limit as mentioned earlier.

In all cases, the most important parameter for the dead zone size is the surface mass density of the disk at 1 AU Σ_0 . Both Re_M and α_{ss} also have a large effect on the dead zone size, while the environmental effect on the dead zone seems to be negligible unless the X-ray ionization from external sources is very powerful.

4.2 Clustered vs Isolated Star Formation – Planetary Gap-opening Masses

The general effect of a dead zone upon planetary masses is to create a bimodal distribution. Gap-opening masses will be sharply reduced as we move inwards through the well-coupled outer region of a disk and encounter the dead zone. This is shown in Fig. 4 which plots the gap-opening mass as a function of disk radius by assuming $\alpha_{ss} = 0.01$ in the active region. The figure shows the gap-opening mass for the case of $\alpha_{ss} = 0.01$ throughout the disk (upper dashed curve), as well as that for the case of inviscid disks (lower dashed curve). The actual distribution is the heavy black curve, which follows the low, inviscid curve in the dead zone, and then precipitously jumps up to the upper curve in the active, well-coupled outer region of the disk. The maximum mass of a planet in the disk’s dead zone is $M_{\text{max,DZ}} \sim 0.09M_J$ in this example. Just outside of the dead zone, the minimum mass in the well-coupled active zone is $M_{\text{min,AZ}} \sim 0.79M_J$.

We generalize this approach in Fig. 5 which shows gap-opening masses as a function of a disk radius for disks in a cluster (left panels) and isolated disks (right panels). In each panel, we plot the gap-opening mass lines for disks with different, constant values of α_{ss} (1.0, 0.1, 0.01 and 0.001) as

well as Rafikov’s inviscid case (see Equation (2)). The dead zone radius for a disk with each value of α_{ss} depends on the Reynolds number Re_M (MP05). Thus, a cross appears on each $\alpha_{ss} = \text{constant}$ curve, which locates the dead zone radius for that particular disk model. Since we show the data for these 3 different values of Re_M , each panel of this figure has 3 nearly vertical lines, which represent the locus of dead zone radii for all disk models for each value of Re_M . These loci show that the dead zone radii are not highly sensitive to the precise value of the magnetic Reynolds number Re_M .

The reader may construct the predicted gap-opening masses for any disk model (characterized by a value for α_{ss} in the well-coupled active zone, magnetic Reynolds number, surface mass density, and ionization) by choosing the panels in Fig. 5 to construct a figure akin to that of Fig. 4. One of the examples of gap-opening masses throughout the disk is plotted in a heavy black line in each panel. Also plotted is a mass inside a Hill radius (see Equation (1)) which is probably an upper limit for a gap-opening mass in an inviscid disk. This line also gives a rough estimate of planetary masses formed via disk instability. If the disk’s viscosity is larger than ~ 0.01 , these planets are expected to keep on accreting gas after their formation.

An important implication of the results is that Jupiter or more massive planets cannot be formed inside a dead zone (within $\sim 10 - 20$ AU) through core accretion, because a gap opens for much lower mass planets – even for terrestrial planets. These panels also indicate that an inviscid region in a typical protostellar disk gives the same gap-opening masses as those expected in a viscous disk with $\alpha_{ss} = 10^{-4} - 10^{-5}$. Therefore, disks with $\alpha_{ss} = 10^{-4} - 10^{-5}$ can be treated as dead.

Another implication of Fig. 5 is that super massive Jovian planets are difficult to form. For example, to obtain $10M_J$ within a reasonable radius ~ 40 AU, the required viscosity parameter is $\alpha_{ss} = 0.1$ for a clustered environment and ~ 1 for an isolated environment. Therefore, we speculate that those massive planets may be formed directly through the gravitational instability of the disk, or they could accrete much more gas as they migrate. Regarding the latter case, a moving planet is shown not to deplete its feeding zone as much as a static planet (e.g. Rafikov 2002; Alibert et al. 2004).

We saw in Fig. 4 that the bimodal character of planetary masses created by dead zones can be characterized by a large jump in planetary masses; $M_{\text{max,DZ}} \rightarrow M_{\text{min,AZ}}$. Fig. 6 shows this jump in gap-opening masses just inside and outside the dead zone radii. For each value of Re_M and α_{ss} , the dead zone radii seen in Fig. 3 can be combined with gap-opening masses in Fig. 5 to produce Fig. 6. These panels clearly show there is a jump in mass at the edge of a dead zone. Since dead zone sizes are more or less the same in both clustered and isolated environments (see Fig. 3), and since gap-opening masses around typical dead zone radius (a few tens of AU) are about the same (see Fig. 5), these minimum and maximum gap-opening masses at a dead zone radius are about the same for both clustered and isolated star-forming environments.

For a heavier disk with $\Sigma_0 = 10^4 \text{ g cm}^{-2}$ (right panels), the “minimum” and “maximum” gap-opening mass lines intersect for a small viscosity parameter of $\alpha_{ss} \sim 10^{-3}$. This is because gap-opening masses for an inviscid disk exceeds

those for a viscous disk for a sufficiently small value of α_{ss} (see the intersection of the lower two curves in the lower panels of Fig. 5). Therefore, in a moderately heavy disk with $\alpha_{ss} \leq 10^{-3}$, there is no jump in gap-opening masses.

Environmental effects on gap-opening masses can also be seen in these heavier mass disk cases. In the upper right panel of Fig. 6, where the dead zones are calculated by the total ionization, gap-opening masses are significantly different compared to the corresponding case for $\Sigma_0 = 10^3 \text{ g cm}^{-2}$ (upper left panel), despite the fact that the dead zone sizes are about the same in both environments in both cases. This implies the difference in gap-opening masses between two environments seem more significant in a heavier disk. This is because dead zone radii for $\Sigma_0 = 10^4 \text{ g cm}^{-2}$ is about 20–50 AU, while those for $\Sigma_0 = 10^3 \text{ g cm}^{-2}$ is about 10–25 AU, and because environmental effects kick in only beyond ~ 10 AU. Another example is a heavy disk ionized only by X-rays (lower right panel). Here, gap-opening masses in two environments give more or less the same values. However, note that we are comparing these masses at very different dead zone radii – for example, for $(Re_M, \alpha_{ss}) = (10^3, 0.01)$, the dead zone radius is 36 AU for a clustered environment and 61 AU for an isolated environment. Therefore, these results imply that gap-opening masses in an isolated environment is changing less sharply, as we can see in Fig. 5.

In the left panel of Fig. 7, we compare gap-opening masses at 20 AU in clustered and isolated star-forming regions. The gap-opening masses in a clustered environment are about a factor of 1.5 larger than the ones in an isolated environment. For standard viscosity parameters $\alpha_{ss} = 10^{-3} - 0.1$, the gap-opening masses change from roughly a Saturn mass to a few Jupiter masses at 20 AU. This indicates the importance of the viscosity parameter on a gap-opening mass.

In the right panel of Fig. 7, we plot the gap-opening mass ratios of clustered and isolated environments for both viscous (heavy line, see Equation (4)) and inviscid (light line, see Equation (2)) cases. Note that the result for a viscous case is independent of an actual value of a viscosity parameter. Different star-forming regions change a planetary gap-opening mass by a factor of $\sim 1.2 - 2.8$ beyond 10 AU in both viscous and inviscid disks. This result further confirms that the environmental difference is probably not a large factor in determining gap-opening masses.

4.3 Grain Evaporation in the Inner Disk

Until now, we have neglected the effect of grain evaporation at a high temperature region within the innermost region of an accretion disk. We take account of grains’ thermal evaporation temperature ($T = 1750$ K for graphite grains, $T = 1400$ K for silicate grains; Hillenbrand et al. 1992), and calculate the size of a dead zone for $Re_M = 10^3$ cases. The dead zones now look as in Fig. 8. We have an inner active region due to thermal collisions of alkali ions besides the lack of grains in that region. The corresponding gap-opening masses are plotted in Fig. 9. Note that in situ planet formation in the inner active region ($r \leq 0.04$ AU) is unlikely. This is because the region has no dust (therefore core accretion scenario is impossible) and is gravitationally stable (therefore disk instability scenario is impossible). This inner turbulent

region is likely to accrete onto the star rather quickly and form an inner hole due to a higher viscosity.

5 DEAD ZONES AND PLANETARY MIGRATION

In §1, we argued that the dead zones can slow down planetary migration. Since the type I migration does not depend on a disk's viscosity, the dead zones cannot directly affect the low mass planet migration. However, when a low mass planet starts its migration from outside the dead zone, it can be strongly affected by the existence of the dead zone. This is because of the difference in disk evolution speed between a dead and an active zone. Due to the smaller viscosity in a dead zone, the disk mass accreting toward the central star from an active zone is likely to be accumulated at the edge of the dead zone (Gammie 1996). If a migrating planet sees this denser region, the inner torque could be comparable to, or even greater than, the outer torque in magnitude. This will stall the planet, or even reverse its migration. As we argued in §1, the type I migration of a non-gap-opener can in principle be divided into two groups: (1) when there is enough mass accumulation at the edge of a dead zone, a protoplanetary migration is either stalled or reversed, and (2) when there is not enough mass accumulation, a planet will migrate into a dead zone and likely to open a gap.

Roughly speaking, for a planet to enter a dead zone without being stopped by the mass accumulation at the dead zone edge, it has to migrate fast enough compared to the disk's mass at around the edge of a dead zone. Fig. 10 compares type I migration timescales of Jupiter, Saturn, 10 Earth mass planet, and Earth (heavy lines, from bottom to top) with disk's viscous evolution timescales (or equivalently type II migration timescales) for $\alpha_{ss} = 1 - 10^{-5}$ (light lines, from bottom to top). Here we used the following timescale equations (Terquem 2003)

$$\tau_{\text{I}} \sim 10^{10} \left(\frac{M_p}{M_E}\right)^{-1} \frac{1}{\Sigma\sqrt{r}} \left(\frac{h_p}{r_p}\right)^2 \quad (5)$$

$$\tau_{\text{II}} = \frac{1}{3\alpha_{ss}} \left(\frac{h_p}{r_p}\right)^{-2} r^{3/2}, \quad (6)$$

where M_E is the Earth mass. For $\alpha_{ss} = 0.01$, it is apparent that Saturn or more massive planets migrate much faster than disk's mass while 10 Earth mass or lighter planets migrate slower. We expect that this mechanism may keep lighter planets beyond a dead zone and help them to grow larger.

A dead zone's effect on type II migration can be readily seen in Fig. 10. For example at 10 AU, the migration timescale is $> 10^4$ years for $\alpha_{ss} = 0.01$ (in an active zone), and $> 10^6$ years for $\alpha_{ss} = 10^{-4}$ (in a dead zone). Thus, type II planets slow down significantly as soon as they enter the dead zone due to the lower viscosity there.

6 DEAD ZONES AND PLANETARY ECCENTRICITY

One of the major surprises about extrasolar planetary systems is the presence of isolated planets with large orbital

eccentricities. Moreover, all very massive extrasolar planets ($M_p > 7M_J$) found so far have rather large eccentricities ($e > 0.2$). We argue that this phenomenon may also be explained by the existence of a dead zone.

Current models suggest that the growth of planetary eccentricity takes place while the disk is still present. In such a situation, eccentricity evolution can occur either through planet-planet interaction (e.g. Chiang et al. 2002) or planet-disk interaction (e.g. Goldreich & Sari 2003; Sari & Goldreich 2004, hereafter GS03 and SG04 respectively). Planet-planet interaction would require similar mass (or more massive) planets to enhance their eccentricities, while all systems with a very massive planet do not have such a companion. It is possible that a similar mass companion was ejected out of the system due to a strong interaction. The other possibility – planet-disk interaction – can increase the eccentricity if a planet with an initial mild eccentricity opens a large enough gap (SG04). Since larger gaps are expected in regions of smaller viscosity, we suggest that planets caught in gaps within dead zones are likely to grow their eccentricity.

Conditions during gap formation may be particularly favorable for eccentricity growth of a planet (GS03, SG04). Planetary interaction with disks at Lindblad resonances enhances their eccentricity whereas interaction at corotation resonances damp it. A necessary condition for eccentricity growth therefore is that the non-linear saturation of the corotation resonances occur. This condition implies that the timescale on which the density gradient is flattened by corotation resonance (t_{sat}), is shorter than both the disk viscous timescale (t_{vis}) and the timescale on which the gap of width w is opened by the principal Lindblad resonances (t_{gap}); $t_{sat} < (t_{vis}, t_{gap})$ (SG04). It is also necessary that the eccentricity must grow faster than the gap grows. Slightly modifying their paper, we show that the initial eccentricity has to be at least

$$\begin{aligned} e_{0,\min} &= \max[e_{1,\min}, e_{2,\min}] \quad (7) \\ e_{1,\min} &= \frac{\alpha_{ss}^{2/3}}{M_p/M_*} \left(\frac{M_p}{M_d}\right)^{5/3} \left(\frac{h_p}{r_p}\right)^{4/3} \\ e_{2,\min} &= \left(\frac{M_p}{M_*}\right)^3 \left(20 \left(\frac{M_p}{M_d}\right)\right)^{-7} \end{aligned}$$

for this kind of eccentricity evolution to occur (see Appendix B for the derivation).

Fig. 11 shows a calculated minimum initial eccentricity for Jupiter and 10 Jupiter mass planet in the disk of Fig. 8 with $\alpha_{ss} = 0.01$. It is immediately clear that the required initial eccentricity for very massive planets is very low ($e_{0,\min} \sim 10^{-3}$) inside a dead zone while that outside a dead zone is more than 0.1. This suggests that eccentricity of heavy planets may have been excited inside dead zones through disk-planet interaction as they migrated into them and opened gaps. It is interesting to note that all high eccentricity ($e > 0.2$) planets observed so far, including very massive planets ($M_p > 7M_J$), are found between 0.07 – 10 AU – roughly the region of a dead zone. If a planet's eccentricity is enhanced due to an interaction with a disk, we expect planets with small eccentricities to be found beyond 10 AU.

The condition that $e_{1,\min} = e_{2,\min}$ in Equation (7) gives the absolute minimum of the initial eccentricity required to

excite eccentricity growth. This occurs for roughly a Uranus-mass planet. We can determine the maximum and minimum mass planets whose initially required eccentricity is reasonably small (e.g. $e_0 = 0.01$). By setting $e_{1,\min} = 0.01$, and assuming a disk mass of $M_d = 0.01M_\odot$ as well as a dead zone's viscosity of $\alpha_{ss} = 5 \times 10^{-5}$, we can determine the maximum mass planet whose eccentricity is likely to be excited through planet-disk interaction. We find that all very massive planets (up to $\sim 20M_J$) may grow their eccentricity inside the dead zone in this way. Similarly, by setting $e_{2,\min} = 0.01$, we can determine the minimum mass planet. Our calculation shows that planets less than an Earth-mass in a disk of $M_d = 0.01M_\odot$ are too light to interact with a disk and enhance their orbital eccentricity. Combining these results together, we can see that planets with masses between Earth and 20 Jupiter masses may enhance their eccentricity reasonably easily inside the dead zone.

7 CONCLUSIONS

We calculated the sizes of dead zones and gap-opening masses in models of stationary protostellar disks. We performed an extensive parameter search: $\Sigma_0 = 10^3 - 10^4 \text{ g cm}^{-2}$, $\alpha_{ss} = 10^{-3} - 1$, $Re_M = 10^2 - 10^4$, and compared (1) disks in a clustered environment and isolated disks, and (2) disks with and without cosmic ray ionization. Our major findings are as follows:

(i) Dead zones are robust features of protostellar disks. We took account of all the major sources of ionization and recombination and considered other effects like ambipolar diffusion and mass mixing between active layers and a dead zone. We showed that dead zones typically stretch out to a few tens of AU.

(ii) Cosmic ray ionization has a large effect on an ionization structure at outer part of the disk (beyond 10 AU), but does not change the sizes of dead zones significantly. From Fig. 2, it is clear that the ionization of an outer part of the disk is dominated by cosmic rays. The sizes of dead zones determined by the total ionization and those by the X-ray ionization are about the same for the same parameter set (Σ_0 , α_{ss} , Re_M), in the same environment (clustered or isolated star-forming regions), because the ionization structure in inner dense regions are similar (i.e. dead zone boundaries intersect with a critical mass ratio at similar radii). The difference due to ionization sources become more apparent in a denser disk ($\Sigma_0 \geq 10^4 \text{ g cm}^{-2}$) because disks become more optically thick.

(iii) The size of a dead zone depends mildly on magnetic features of a disk (α_{ss} and Re_M), and rather strongly on a disk surface mass density Σ_0 (see Fig. 5). It is almost independent of disk's environments (clustered or isolated star-forming regions).

(iv) Jovian or super Jovian planets are likely to be formed beyond a dead zone. Inside dead zones, a gap opens for smaller mass planets – ice giants or even terrestrial planets (see Fig. 4 and 5).

(v) Dead zones may significantly slow down both type I and type II planet migration (see §5).

(vi) Gaps within the dead zones may be good regions in which planets enhance their orbital eccentricities via planet-

disk interaction. As we discussed in §6, this may be especially true for very massive planets ($M_p > 7M_J$).

In our future work, we revisit the problem of planetary migration and dead zones by using time-dependent calculations.

ACKNOWLEDGMENTS

We thank Eric Feigelson, David Hollenbach, Doug Lin, Edward Thommes and James Wadsley for stimulating discussions. We also thank an anonymous referee, Shu-ichiro Inutsuka, and Jim Pringle for useful comments. S. M. is supported by a SHARCNET Graduate Fellowship while R. E. P. is supported by a grant from the National Science and Engineering Research Council of Canada (NSERC).

REFERENCES

- Alibert Y., Mordasini C., Benz W., 2004, *A&A*, 417, L25
 Balbus S. A., Hawley J. F., 1991, *ApJ*, 376, 214
 Boss A. P., 1997, *Science*, 276, 1836
 Chiang E. I., Fischer D., Thommes E., 2002, *ApJL*, 564, L105
 Chiang E. I., Goldreich P., 1997, *ApJ*, 490, 368
 Chiang E. I., Joungh M. K., Creech-Eakman M. J., Qi C., Kessler J. E., Blake G. A., van Dishoeck E. F., 2001, *ApJ*, 547, 1077
 Desch S. J., Connolly H. C., Srinivasan G., 2004, *ApJ*, 602, 528
 Feigelson E. D., Broos P., Gaffney J. A., Garmire G., Hillenbrand L. A., Pravdo S. H., Townsley L., Tsuboi Y., 2002, *ApJ*, 574, 258
 Fleming T., Stone J. M., 2003, *ApJ*, 585, 908
 Fleming T. P., Stone J. M., Hawley J. F., 2000, *ApJ*, 530, 464
 Fromang S., Terquem C., Balbus S. A., 2002, *MNRAS*, 329, 18
 Gammie C. F., 1996, *ApJ*, 457, 355
 Glassgold A. E., Feigelson E. D., Montmerle T., 2000, *Protostars and Planets IV*. The University of Arizona Press, 2000
 Goldreich P., Sari R., 2003, *ApJ*, 585, 1024
 Goldreich P., Tremaine S., 1980, *ApJ*, 241, 425
 Hawley J. F., Stone J. M., 1998, *ApJ*, 501, 758
 Hillenbrand L. A., Strom S. E., Vrba F. J., Keene J., 1992, *ApJ*, 397, 613
 Hollenbach D., Johnstone D., Lizano S., Shu F., 1994, *ApJ*, 428, 654
 Inutsuka S., Sano T., 2005
 Kley W., 1999, *MNRAS*, 303, 696
 Lepp S., 1992, in *IAU Symp. 150: Astrochemistry of Cosmic Phenomena The Cosmic-Ray Ionization RATE**. pp 471–+
 Lin D. N. C., Papaloizou J. C. B., 1993, *Protostars and Planets III*. The University of Arizona Press
 Lubow S. H., Seibert M., Artymowicz P., 1999, *ApJ*, 526, 1001
 Lufkin G., Quinn T., Wadsley J., Stadel J., Governato F., 2004, *MNRAS*, 347, 421

- Luhman K. L., Briceño C., Stauffer J. R., Hartmann L., Barrado y Navascués D., Caldwell N., 2003, *ApJ*, 590, 348
- Matsumura S., Pudritz R. E., 2003, *ApJ*, 598, 645
- Matsumura S., Pudritz R. E., 2005, *ApJL*, 618, L137
- Mayer L., Quinn T., Wadsley J., Stadel J., 2002, *Science*, 298, 1756
- Press W. H., Teukolsky S. A., Vetterling W. T., Flannery B. P., 1996, *Numerical Recipes in Fortran*. Cambridge: Cambridge University Press
- Rafikov R. R., 2002, *ApJ*, 572, 566
- Robberto M., Beckwith S. V. W., Panagia N., 2002, *ApJ*, 578, 897
- Sano T., Miyama S. M., Umebayashi T., Nakano T., 2000, *ApJ*, 543, 486
- Sano T., Stone J. M., 2002, *ApJ*, 577, 534
- Sari R., Goldreich P., 2004, *ApJL*, 606, L77
- Shakura N. I., Sunyaev R. A., 1973, *A&A*, 24, 337
- Shu F. H., Johnstone D., Hollenbach D., 1993, *Icarus*, 106, 92
- Skilling J., Strong A. W., 1976, *A&A*, 53, 253
- Stelzer B., Flaccomio E., Montmerle T., Micela G., Sciortino S., Favata F., Preibisch T., Feigelson E. D., , 2005
- Terquem C. E. J. M. L. J., , 2003
- Thommes E. W., 2005, *ApJ*, 626, 1033
- Umebayashi T., Nakano T., 1981, *PASJ*, 33, 617
- Ward W. R., 1997, *Icarus*, 126, 261

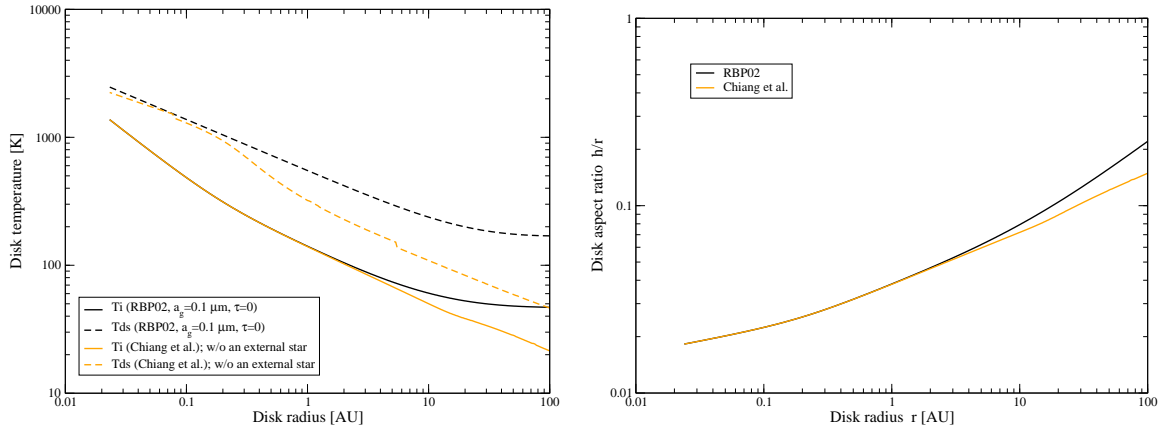


Figure 1. Left: temperature structures of disk models in clustered (heavy lines) and isolated (light lines) environments. Solid lines show disk temperatures below the pressure scale height of the disk, and dashed lines show disk envelope’s temperatures. Right: disk aspect ratios of disk models in clustered (heavy line) and isolated (light line) environments. External fields’ effects become important in an outer part of the disks.

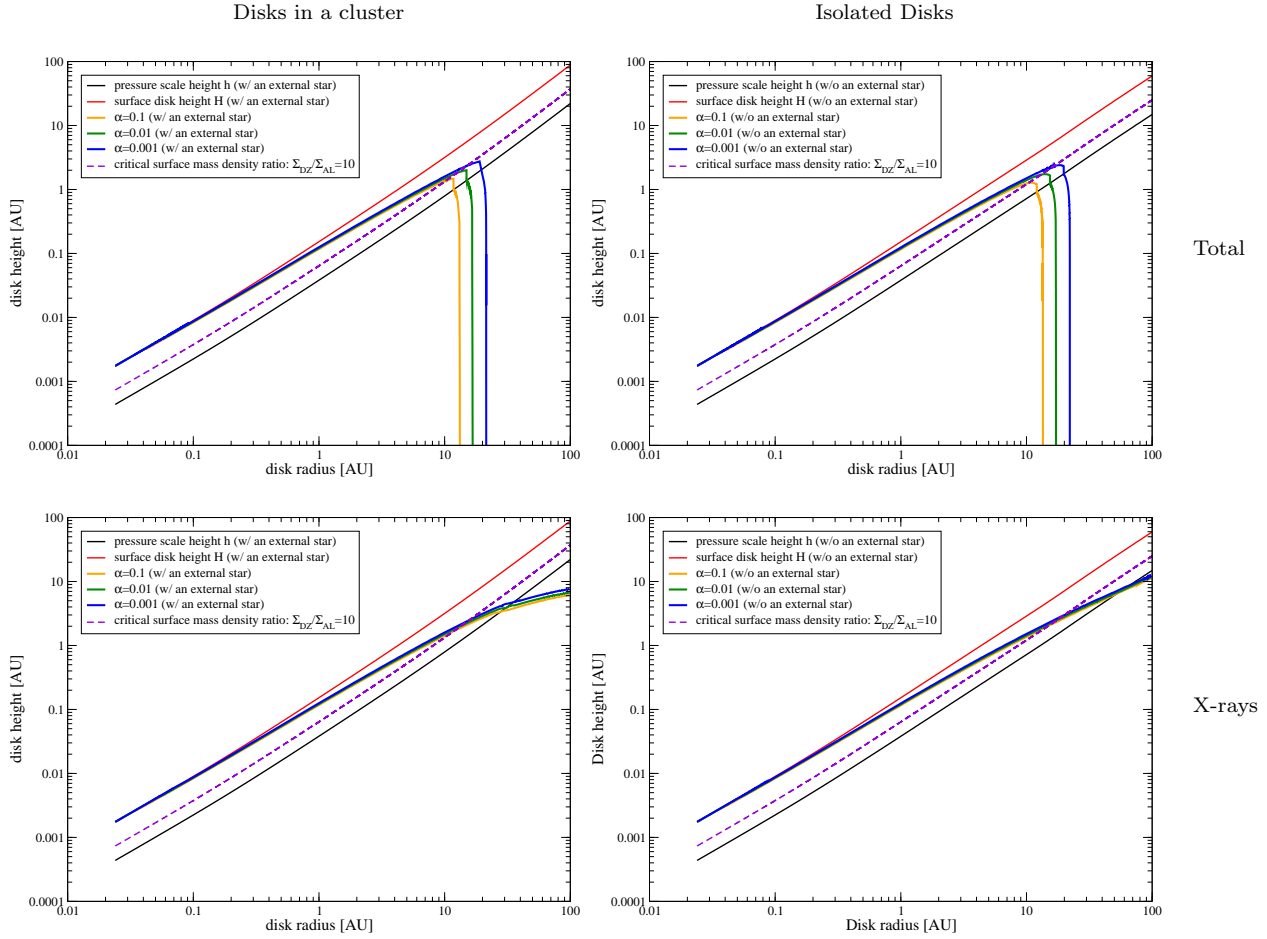


Figure 2. Comparing dead zones in clustered (left panels) and isolated (right panels) environments. For the upper panels, ionization sources are X-rays from the magnetosphere of a central star and an external star (for a disk in a clustered environment) as well as cosmic rays, radioactive elements, and thermal ionization by alkali ions. For the lower panels, the ionization sources are X-rays from the magnetosphere of a central star and an external star (for a disk in a clustered environment). Here, we choose $\Sigma_0 = 10^3 \text{ g cm}^{-2}$ with $Re_M = 10^3$. The uppermost line shows the surface disk height; the lowermost line shows the pressure scale height, while three curves indicate the dead zone boundaries for $\alpha_{ss} = 0.1, 0.01,$ and 0.001 from inside to outside. The dashed line is where $\Sigma_{\text{below}}/\Sigma_{\text{above}} = 10$.

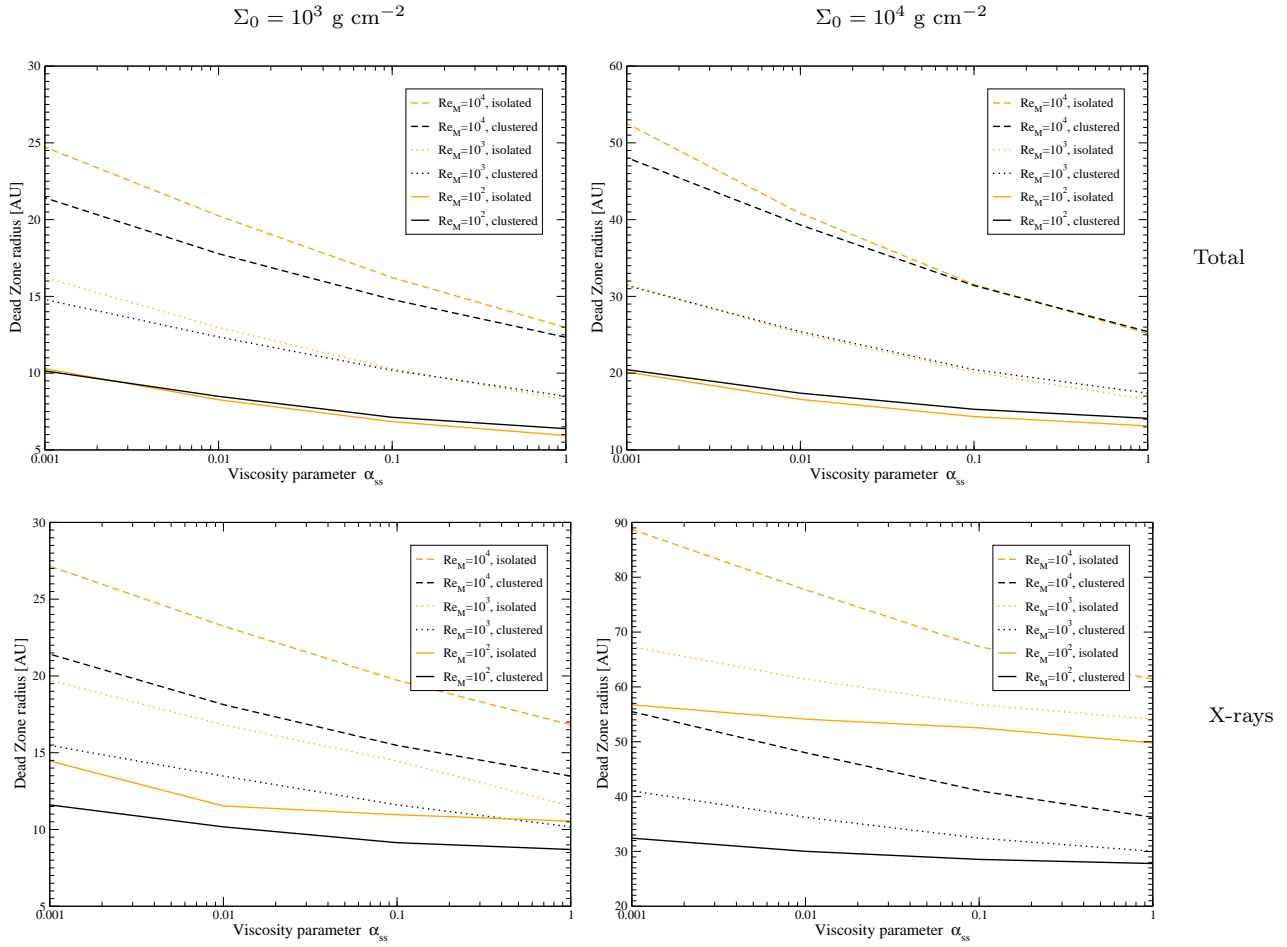


Figure 3. Comparing dead zone radii in clustered (heavy lines) and isolated (light lines) environments. Solid, dotted and dashed lines are for $Re_M = 10^2$, 10^3 , and 10^4 respectively. The difference between two environments are more apparent in the cases without cosmic ray ionization (lower panels) compared to general cases (upper panels). Note the difference in scale of the y axes.

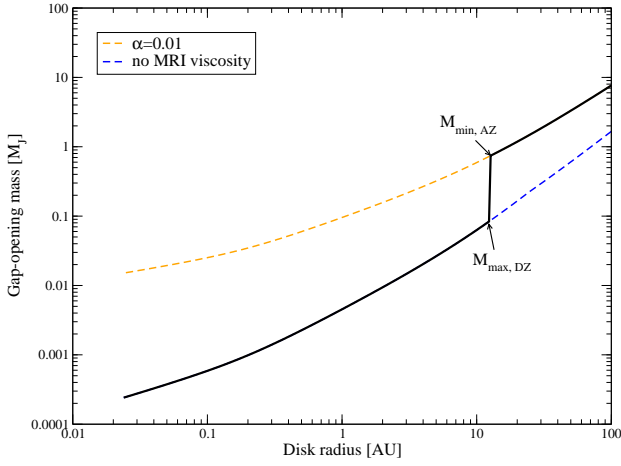


Figure 4. Gap-opening masses for a disk exposed to an external star which has the surface mass density, at 1 AU, of $\Sigma_0 = 10^3 \text{ g cm}^{-2}$. The lower dashed line shows the gap-opening mass for the case of no MRI viscosity, while the upper dashed line shows the gap-opening masses for $\alpha_{ss} = 0.01$. For the magnetic Reynolds number $Re_M = 10^3$, the fiducial minimum gap-opening mass throughout the disk is shown in a heavy line.

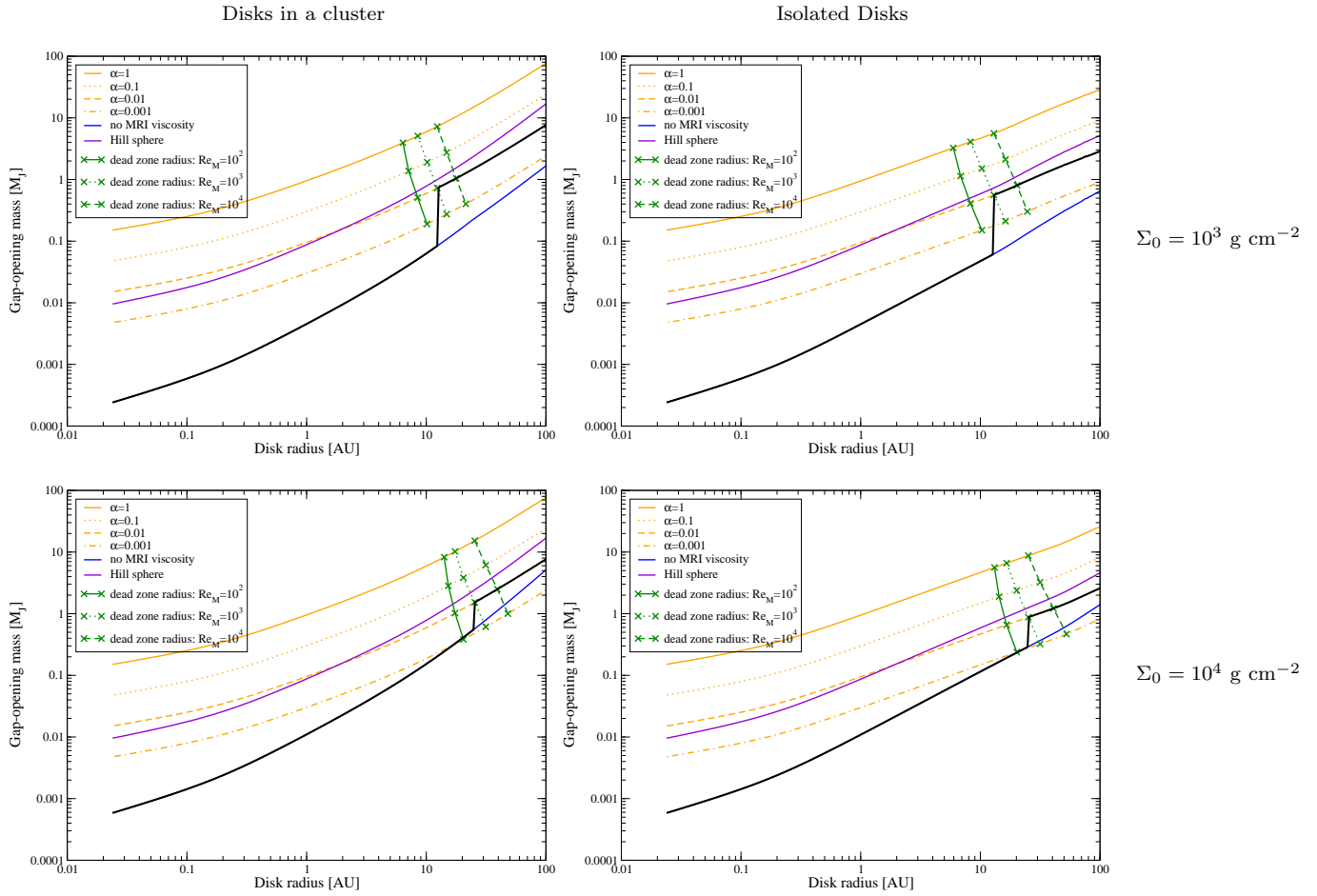


Figure 5. Comparing dead zones in clustered (left panels) and isolated (right panels) environments. Dead zone radii are calculated by using the total ionization rate in all cases. For upper panels, we assume the surface mass density at 1 AU of $\Sigma_0 = 10^3 \text{ g cm}^{-2}$, while for lower panels, $\Sigma_0 = 10^4 \text{ g cm}^{-2}$. The lowermost line shows the gap-opening mass for the case of no MRI viscosity, while the upper parallel lines show the gap-opening masses for a different strength of magnetic field: the solid line is for $\alpha_{SS} = 1$, the dotted line is for 0.1, the dashed line is for 0.01, and the dot-dashed line is for 0.001. The dead zone for the magnetic Reynolds number, $Re_M = 10^2$, is inside a solid line with crosses, that for 10^3 is inside a dotted line with crosses, and that for 10^4 is inside a dashed line with crosses. The thick solid line traces our fiducial minimum gap-opening mass throughout the disk for MRI “viscosity,” $\alpha_{SS} = 0.01$.

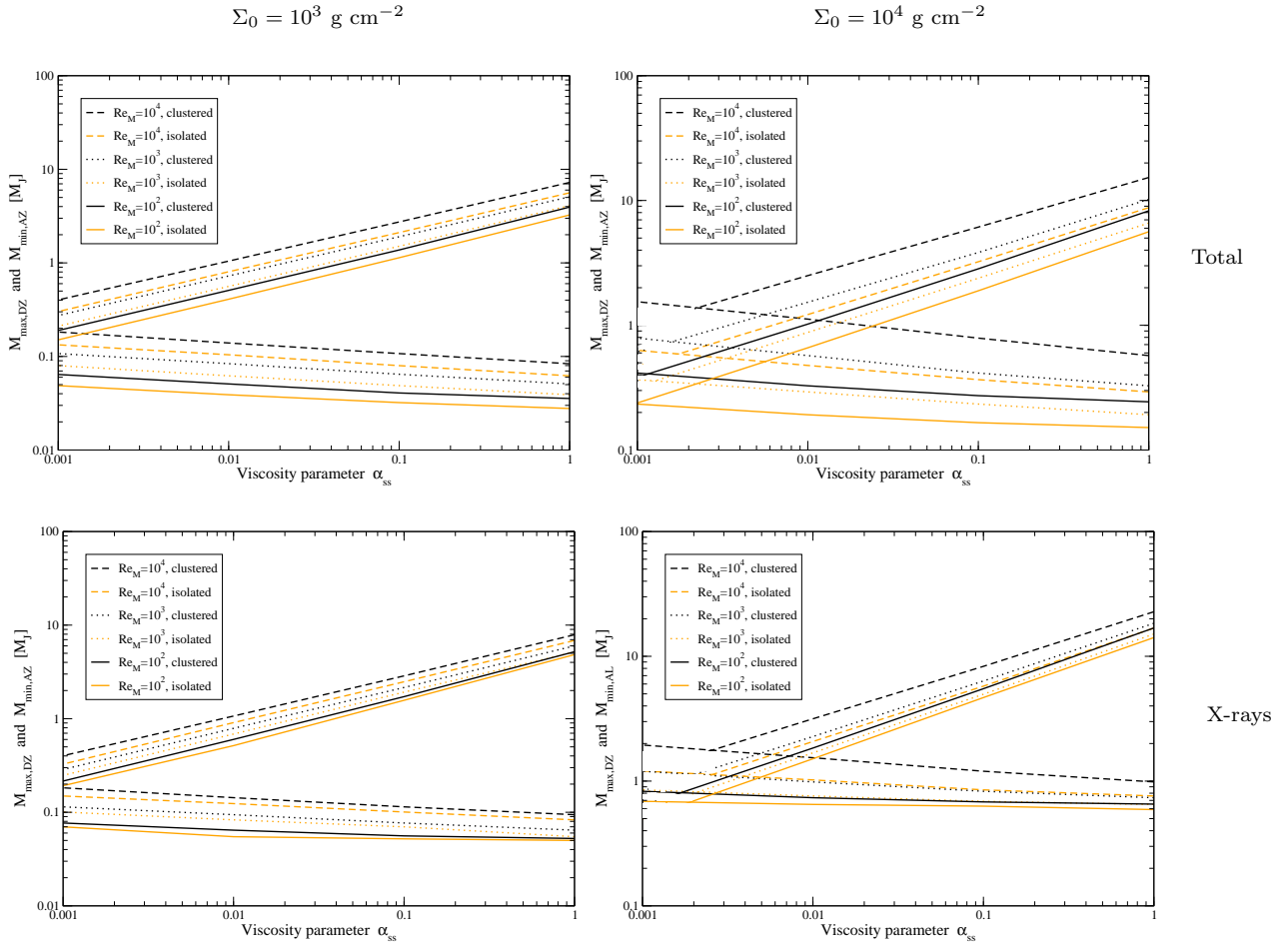


Figure 6. Comparing gap-opening masses just inside and outside the dead zone radii in clustered (heavy lines) and isolated (light lines) environments. Solid, dotted and dashed lines are for $Re_M = 10^2, 10^3$, and 10^4 respectively. The difference between two environments are more apparent in the cases without cosmic ray ionization (lower panels) compared to general cases (upper panels). Note the difference in scale of the y axes.

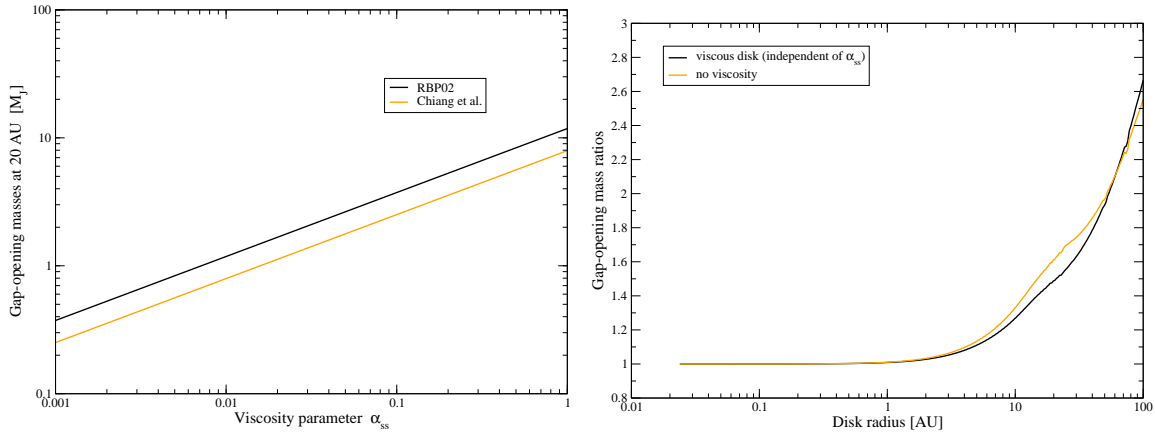


Figure 7. Left: comparison of gap-opening masses at 20 AU in clustered (heavy line) and isolated (light line) environments. Note that the magnetic Reynolds number does not affect the gap-opening masses. Right: gap-opening mass ratios of isolated and clustered star-forming environments. Heavy line is for a viscous disk (see Equation (4)) and light line is for an inviscid disk (see Equation (2)). Note that the results for a viscous disk are independent of a viscosity parameter α_{ss} .

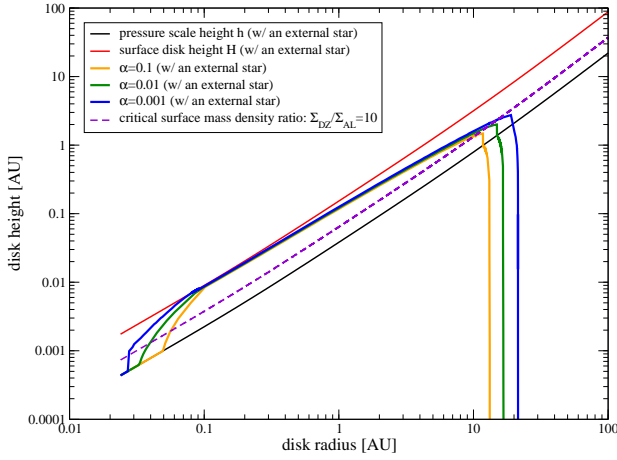


Figure 8. The effect of grain evaporation on the sizes of dead zones calculated for a protostellar disk exposed to an external star. The ionization sources are X-rays from the magnetosphere of a central star and an external star as well as cosmic rays, radioactive elements, and thermal ionization by alkali ions. We use $\Sigma_0 = 10^3 \text{ g cm}^{-2}$ and $Re_M = 10^3$ with $\alpha_{ss} = 0.1, 0.01, \text{ and } 0.001$. For the explanation of each line, see Fig. 2.

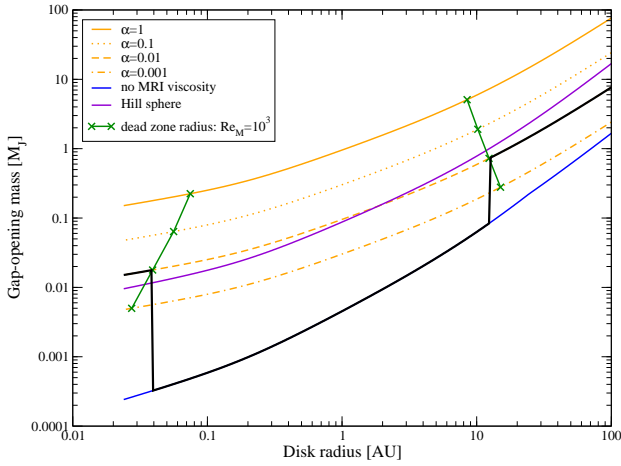


Figure 9. The effect of grain evaporation on gap-opening masses for a disk exposed to an external star which has the surface mass density, at 1 AU, of $\Sigma_0 = 10^3 \text{ g cm}^{-2}$. For the explanation of each line, see Fig. 5.

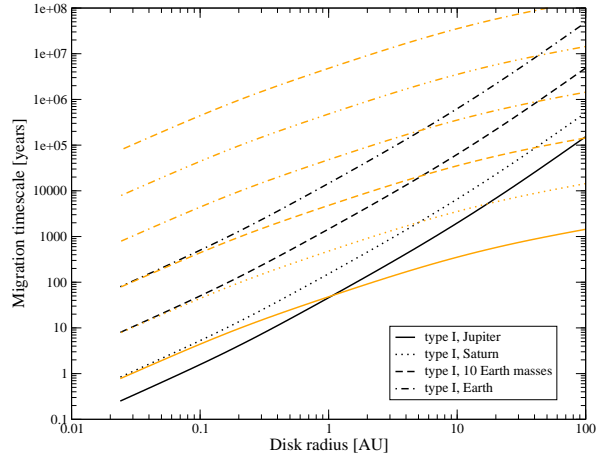


Figure 10. Migration timescales as a function of disk radius. Heavy lines show, from bottom to top, type I migration timescales for Jupiter, Saturn, 10 Earth mass planet, and Earth respectively. Light lines show, from bottom to top, type II migration timescales for $\alpha_{ss} = 1, 0.1, 0.01, 10^{-3}, 10^{-4}, 10^{-5}$ respectively.

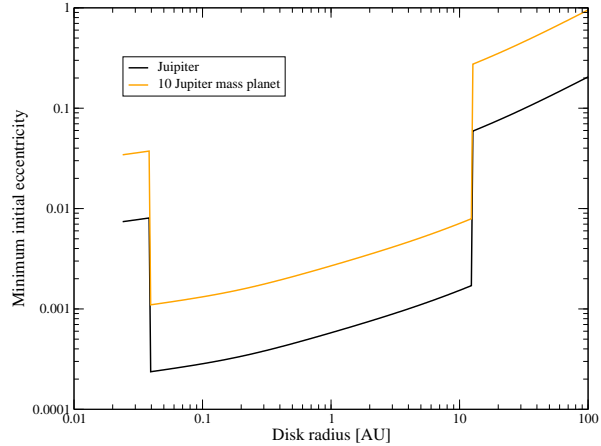


Figure 11. The minimum initial eccentricity required for eccentricity evolution via planet-disk interaction (Goldreich & Sari 2003). Heavy line is for a Jupiter mass planet and light line is for a 10 Jupiter mass planet. Obviously, eccentricity growth is more likely for a planet in the dead zone.

Table 1. Recombination coefficients in rate equations.

symbols	recombination rate coefficients [cm^3s^{-1}]	pairs
β	$3 \times 10^{-6} T^{-1/2}$	electrons – molecular ions
β_r	$3 \times 10^{-11} T^{-1/2}$	electrons – metal ions
β_t	3×10^{-9}	molecular ions – metal atoms
β_1	$\pi a^2 \sqrt{\frac{8k_B T}{\pi m_e}} 0.6$	electrons – neutral grains
β_2	$\pi a^2 \sqrt{\frac{8k_B T}{\pi m_e}} (1 - \frac{q^2}{ak_B T})$	electrons – positively charged grains
β_3	$\pi(2a)^2 \sqrt{\frac{8k_B T}{\pi m_G}} (1 - \frac{q^2}{2ak_B T})$	positively charged grains – negatively charged grains
β_4	$\pi a^2 \sqrt{\frac{8k_B T}{\pi m_m}}$	molecular ions – neutral grains
β_5	$\pi a^2 \sqrt{\frac{8k_B T}{\pi m_m}} (1 - \frac{q^2}{ak_B T})$	molecular ions – negatively charged grains
β_6	$\pi a^2 \sqrt{\frac{8k_B T}{\pi m_M}}$	metal ions – neutral grains
β_7	$\pi a^2 \sqrt{\frac{8k_B T}{\pi m_M}} (1 - \frac{q^2}{ak_B T})$	metal ions – negatively charged grains

APPENDIX A: EFFECT OF GRAINS ON DISK IONIZATION BALANCE

To calculate an electron fraction by including various recombination sources, we write the rate equations for electrons, molecular ions, neutral and singly charged grains as follows:

$$\begin{aligned} \frac{dn_e}{dt} = & \xi n_n - \beta n_{m^+} n_e - \beta_r n_{M^+} n_e - \beta_1 n_G n_e \\ & - \beta_2 n_{G^+} n_e \end{aligned} \quad (\text{A1})$$

$$\begin{aligned} \frac{dn_{m^+}}{dt} = & \xi n_n - \beta n_e n_{m^+} - \beta_t n_M n_{m^+} - \beta_4 n_G n_{m^+} \\ & - \beta_5 n_{G^-} n_{m^+} \end{aligned} \quad (\text{A2})$$

$$\begin{aligned} \frac{dn_G}{dt} = & \beta_2 n_{G^+} n_e + \beta_5 n_{G^-} n_{m^+} + \beta_7 n_{G^-} n_{M^+} \\ & + 2 \beta_3 n_{G^+} n_{G^-} - \beta_1 n_e n_G - \beta_4 n_{m^+} n_G \\ & - \beta_6 n_{M^+} n_G \end{aligned} \quad (\text{A3})$$

$$\begin{aligned} \frac{dn_{G^+}}{dt} = & \beta_4 n_G n_{m^+} + \beta_6 n_G n_{M^+} - \beta_2 n_e n_{G^+} \\ & - \beta_3 n_{G^-} n_{G^+} \end{aligned} \quad (\text{A4})$$

$$\begin{aligned} \frac{dn_{G^-}}{dt} = & \beta_1 n_G n_e - \beta_3 n_{G^+} n_{G^-} - \beta_5 n_{m^+} n_{G^-} \\ & - \beta_7 n_{M^+} n_{G^-} \end{aligned} \quad (\text{A5})$$

$$n_e = n_{m^+} + n_{M^+} + n_{G^+} - n_{G^-} . \quad (\text{A6})$$

Here, n_e , n_m , n_M , n_G , and n_n are the density of electrons, molecules, metals, grains, and neutral hydrogens, while the superscript of + or - indicate the elements are positively or negatively charged respectively. Also, ξ is the total ionization rate β s are recombination rate coefficients (see Table 1 for details). We solve these differential equations together with charge conservation by using a semi-implicit extrapolation method (a generalized Bulirsch-Stoer method) (stifbs.f90 in Press et al. 1996). This calculation takes about a few hours to run on the average workstation.

Table 1 shows all recombination coefficients appeared in above equations, where k_B is the Boltzmann constant, T is the disk temperature, a is a grain radius, and q is the charge. Also, m_e , m_m , m_M , and m_G are the mass of electrons, molecules, metals, and grains respectively. The recombination rate coefficients β , β_r , β_t are taken from Fromang et al. (2002), and the rest are obtained by following the method by Sano et al. (2000).

APPENDIX B: MINIMUM INITIAL ECCENTRICITIES

In §5, we argued that there is the minimum initial eccentricity required to enhance a planetary eccentricity via planet-disk interaction. Sari & Goldreich (2004) suggested that for the eccentricity to grow, (1) the corotation resonances must saturate, and (2) eccentricity must grow faster than a gap opens. Also, they claimed that eccentricity does not significantly decay as long as (3) corotation resonances are more than 5 % saturated.

For the first point, two equations must be satisfied: $t_{sat} < t_{vis}$; which may be written as

$$e > \frac{\alpha_{ss}^{2/3}}{M_p/M_*} \left(\frac{w}{r_p} \right)^{5/3} \left(\frac{h_p}{r_p} \right)^{4/3} \equiv e_1 \quad (\text{B1})$$

as well as $t_{sat} < t_{gap}$; which becomes

$$e > \left(\frac{M_p}{M_*} \right)^3 \left(\frac{r_p}{w} \right)^7 \equiv e_2 \quad (\text{B2})$$

where w is a gap width and M_* is the stellar mass (SG04).

Combining the second and third points, we can write

$$\frac{M_p}{M_d} < \frac{w}{r_p} < 20 \frac{M_p}{M_d} , \quad (\text{B3})$$

where M_d is a disk mass. The left inequality arises because a gap has to open slower than the eccentricity evolution timescale, while the right inequality comes in so that the significant decay won't happen.

Writing these as the minimum and maximum ratios of a gap width and a disk radius, we can rewrite first two conditions as follows:

$$e > e_1 \quad (\text{B4})$$

$$> \frac{\alpha_{ss}^{2/3}}{M_p/M_*} \left(\frac{w}{r_p} \right)_{\min}^{5/3} \left(\frac{h_p}{r_p} \right)^{4/3} \equiv e_{1,\min}$$

$$e > e_2 \quad (\text{B5})$$

$$> \left(\frac{M_p}{M_*} \right)^3 \left(\frac{w}{r_p} \right)_{\max}^{-7} \equiv e_{2,\min} .$$

Thus, the eccentricity must be at least $e > \max [e_{1,\min}, e_{2,\min}]$ to be excited, which is Equation (7).